Effects of Self-Phase Modulation on Sub-500 fs Pulse Transmission over Dispersion Compensated Fiber Links

Shuai Shen, *Member, OSA*, Cheng-Chun Chang, Harshad P. Sardesai, Vikrant Binjrajka, and Andrew M. Weiner, *Fellow, IEEE, Fellow, OSA*

***Abstract*—The effects of nonlinearity on sub-500 fs pulse transmission over dispersion compensated fiber links using dispersion compensating fiber technique are investigated numerically and experimentally. The pulse broadening and recompression ratio of the 2.5-km transmission link is over 300. The postcompensated and precompensated links are compared when the input pulse energy ranges from 15 to 150 pJ. At high powers, self-phase modulation (SPM) degrades the pulse recompression process and provides an upper bound on the transmitted pulse energy. The SPM effect is stronger in the postcompensated link than in the precompensated link. A dramatic spectral narrowing effect was observed in the postcompensated link. Pulse energies up to tens of pJ, consistent with high quality communication, should be possible for a sub-500 fs pulse in such dispersion compensated links.**

***Index Terms*— Dispersion compensation, femtosecond pulses, fiber optics, self-phase modulation.**

I. Introduction

WITH the fiber loss being compensated by the erbium-doped fiber amplifier (EDFA), group velocity dispersion (GVD) and nonlinearities have become major factors in limiting the bandwidth length product of the ultrashort pulse transmission link. Dispersion and dispersion compensation are especially key for high-speed lightwave transmission systems, such as time-division multiplexed (TDM) [1] and code-division multiple access (CDMA) systems [2]. A variety of dispersion compensating techniques have been proposed and investigated recently, e.g., midspan spectral inversion [3]–[5], chirped fiber Bragg gratings [6], [7], bulk grating-and-lens pairs [8], and dispersion compensating fibers (DCF) [9]–[12]. Mostly the purpose of these techniques is to upgrade the embedded standard single-mode fibers (SSMF) which have a large anomalous dispersion ($D = 17$ ps/km/nm) at 1.55 μm. Among these dispersion compensating schemes, the DCF technique is especially attractive for fs-pulse transmission, where the simultaneous compensation of both the second- and the third-order dispersion [or group velocity dispersion (GVD) and dispersion slope] is necessary. A suitable DCF can effectively suppress much of the third-order dispersion of the standard SMF. Meanwhile, this all-fiber compensating scheme can be conveniently implemented in the existing standard SMF transmission link. Recently, simultaneous compensation of the second- and most of the third-order dispersion of SSMF with a special single-mode DCF for a fs pulse transmission have been successfully demonstrated over 42-m and 2.5-km SSMF-DCF concatenated links respectively [10], [13]. Such DCF exhibits both negative dispersion and dispersion slope. The overall residual dispersion of the SSMF-DCF link was shown to be four times lower than that of the dispersion shifted fiber (DSF).

In a DCF compensating system, the bandwidth length product of the transmission link is no longer limited by the GVD but by higher order dispersion and nonlinear effects. The dominant nonlinear effect in the TDMA and CDMA optical fiber systems is the self-phase modulation effect (SPM), which is caused by the nonlinear dependence of the refractive index on pulse intensity. Since high-speed data transmission systems require greater received power for error-free detection, the performance of ultrashort pulse dispersion compensated link is eventually limited by the interaction of SPM and the fiber dispersion. Hence, it becomes necessary to investigate the nonlinear effects on a dispersion compensated link for a complete understanding of the limitation of the DCF compensating technique in a fs-pulse transmission system. Previously, the SPM effects on the dispersion compensated link with DCF were studied only in the sub-10 to 100 ps range [14]–[18]. As the pulse width of the transmission link is continuously decreased into fs regime, the pulse broadening and recompression factor will be drastically increased. The cubic phase will also be significantly increased. Detailed analysis on the interaction among SPM and second- and third-order dispersion for fs-pulse transmission is necessary. The intent of our work is to explore the limit incurred by nonlinear effects for such dispersion compensated fiber links with extremely large pulse stretching and recompression factors for fs-pulses. The goal is to determine whether dispersion compensated linear pulse propagation is possible at power levels suitable for high-quality lightwave transmission. Our work emphasizes

Manuscript received June 29, 1998; revised November 24, 1998. This work was supported by the National Science Foundation under Grants ECS-9626967 and ECS-9312256.

S. Shen and A. M. Weiner are with the School of Electrical and Computer Engineering, Purdue University, West Lafayette, IN 47907 USA.

C.-C. Chang is with Bell Laboratories, Lucent Technology, Holmdel, NJ 07733 USA.

H. P. Sardesai is with the Lightwave System Department, Ciena Corporation, Linthicum, MD 21090 USA.

V. Binjrajka is with the Wireless Network Division, Hughes Network Systems, Germantown, MD 20876 USA.

Publisher Item Identifier S 0733-8724(99)01891-5.

isolated fs-pulses, although some calculations on TDM pulse transmission are also presented.

In this paper, we report a numerical and experimental study of SPM effects on a dispersion compensated link with DCF for sub-500 fs pulse transmission. We model the dispersion balance and SPM effects in our SSMF-DCF and DCF-SSMF links with the nonlinear Schrodinger (NLS) equation. A modified Fourier-split-step algorithm was developed with variable timing windows to increase the simulation speed. Simulations were performed in both precompensated and postcompensated transmission links for isolated input pulses. SPM effects on TDM transmission of pseudorandom data were also simulated. The degradation of dispersion compensation due to the interaction between the SPM effect and the fiber dispersion was demonstrated in experiments over a 2.5-km dispersion compensated link for isolated 400 fs full-width at half maximum (FWHM) input pulses with a pulse broadening and recompression ratio over 300. The power dependent output pulsewidth was investigated and compared for both precompensated and postcompensated scenario within an input energy range from 15 to 150 pJ. In the postcompensated scenario, the delicate dispersion balance was disturbed by the SPM effect significantly. A dramatic spectral narrowing effect was observed at the output of the fiber link. In contrast, the SPM effects in the precompensated scenario are not appreciable. The experiment results are in excellent agreement with the simulation prediction. Our results provide more insight about the interaction between SPM effects and fiber dispersion in the fs-pulse regime and help us to define the power limit in the ultrashort pulse dispersion compensated fiber links.

II. Theoretical Model

At modest input energy level, single-mode fiber behaves as a dispersive, linear medium. The transmitted spectrum does not change during propagation. The pulse becomes weaker due to attenuation and broadened in the time domain by the second order and the third-order dispersion. In an fs-pulse dispersion compensated link consisting of a standard SMF and a dispersion compensating fiber, input pulses are first spread very substantially (e.g., by factors of one hundred or more) as they propagate over a fiber span up to several kilometers. They are subsequently recompressed to their original pulse duration due to the dispersion and dispersion slope balance between SSMF and DCF. Potentially, the dispersion limited propagation distance for subpicosecond pulses in the dispersion compensated link could significantly exceed that possible with soliton propagation which is limited by the soliton self-frequency shift [19]. As the input energy for fs-pulse transmission is increased beyond several tens of picojoules, the fiber nonlinear effect, especially SPM, must be included to describe the pulse dynamics in the transmission link. Our theoretical analysis is to study the nonlinear effects on such dispersion compensated fiber links. In particular, we perform numerical simulations to determine the input power levels at which SPM effects disturb the balance between the SSMF and DCF.

The model used for our simulations is shown in Fig. 1. For the postcompensated link, DCF is connected at the end

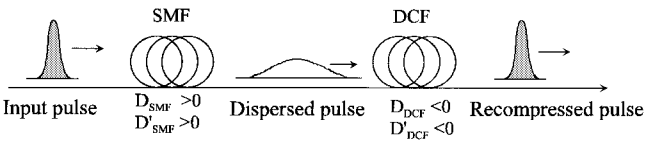

Fig. 1. Simulation model for a postcompensated link. Dispersion compensating fiber acts as a dispersion compensator. D and D' are the dispersion and dispersion slope parameters of the fiber.

of SSMF. By optimizing the length ratio of SSMF to DCF, we can design a transmission link where the DCF provides an exactly equal and opposite second-order dispersion to that in the SSMF. Therefore the second order dispersion recompression is ideal in our model. By simply reversing the order of SSMF and DCF, i.e., the SMF is connected at the end of the DCF, we can model a precompensated fiber link in our analysis. A small residual third-order dispersion of the compensated link caused by a minor dispersion slope mismatch can also be considered to match the experimental conditions. As the input power is increased, SPM modifies the chirp picked up in the fiber, and degrades the recompression process. We concentrate our analysis on the propagation of isolated ultrashort pulses with pulsewidth in the sub-500 fs range. Our approach can be extended to cover code-division multiple-access (CDMA) systems where each pulse is spectrally encoded [20]. It is also relevant to bulk [21] as well as fiber-based [22] chirped pulse amplifier systems in which nonlinear effects can severely impact the compressibility of the amplified pulse.

The nonlinear Schrodinger equation (NLSE), modified to include higher-order dispersion, has been successful in accurately modeling pulse propagation in single-mode fibers in many diverse applications [23], [24]. It can therefore be employed with confidence for dispersion compensated link. In our analysis, we use the normalized NLSE

$$i\frac{\partial U}{\partial \xi} = \operatorname{sgn}(\beta_2)\frac{1}{2}\frac{\partial^2 U}{\partial \tau^2} + \frac{i\beta_3}{6|\beta_2|T_0}\frac{\partial^3 U}{\partial \tau^3} - N^2|U|^2U\exp(-\alpha\xi L_d) \quad (1)$$

where $\xi = z/L_d$ and $\tau = (t - z/v_g)/(T_0)$ represent the normalized distance and retarded time variables, respectively. U is the normalized amplitude such that the amplitude of pulse envelope equals to $\sqrt{P_0}\exp(-\alpha z/2)U(z,\tau)$. P_0 is the peak power of the input pulse and T_0 is the input pulsewidth. β_2 and β_3 are the dispersion and dispersion slope parameters of the fiber respectively. α is the fiber loss coefficient. The dispersion length $L_d = T_0^2/|\beta_2|$ and the nonlinear length $L_{NL} = 1/\gamma P_0$ provide the length scales over which the dispersion and the nonlinear effect become important respectively. γ is the nonlinear coefficient and is related to n_2 and the effective core area A_{eff} by $\gamma = n_2\omega_0/CA_{\text{eff}}$. The ratio of L_d to L_{NL} gives the nonlinearity factor $N^2 = L_d/L_{NL} = \gamma P_0 T_0^2/|\beta_2|$. The index parameter N is normally used to compare the importance of the dispersion and SPM effects in the fiber [25]. Larger N, contributed either from larger input peak power at a fixed pulsewidth or from larger pulsewidth at a fixed peak power, corresponds to larger SPM effects in the fiber link. When $N = 1$, the peak power and pulsewidth

support the fundamental soliton for $\beta_2 < 0$. In our model, we consider the second- and third-order dispersion effects and include SPM as the source of nonlinear terms. Other higher-order nonlinear effects such as the Raman contribution to the nonlinear refractive index and the shock term have been neglected. Since the input power level in our analysis is below that for soliton generation ($N < 1$), the effect of SPM is moderate. As long as we avoid very short pulses ($\leq$100 fs), the Raman effect and shock term, which are usually smaller than SPM, should be negligible. We have performed some simulations including the Raman term for 100 fs pulses for a fiber length up to $1000L_d$. The result shows no appreciable difference compared to simulations without the Raman term. This justifies the neglect of the Raman term for most of the simulations presented here. Brillouin scattering has also been assumed to be suppressed since the optical bandwidth, on the order of terahertz for sub-500 fs pulses, is orders of magnitude larger than the Brillouin linewidth.

III. Numerical Simulation with the Second-Order Dispersion and the SPM Effect

The split-step Fourier transform algorithm is adopted in our simulation. In order to achieve high accuracy with significantly increased computation speed for the simulation of an isolated input pulse, we devised an algorithm to dynamically change the array size and time window of the pulse as it broadens along the fiber. The algorithm checks for the intensity of the pulse at the edge of the window. When the pulse is broadened and the intensity at the edge rises to within 40 dB of the peak power, the array size and the time window are doubled. When the pulse is recompressed and the time-window edge intensity falls below 40 dB, the array size and time window is reduced back by half. In the case of TDM input bit streams, the array size is fixed since the bit stream fills the time window completely even at the beginning of the fiber. In our calculation, the array size used to represent the input pulse was 64 with a time window of $10T_0$. It increased to array size of 65 536 over a time window of $10\,240T_0$ for the propagation distance of $1000L_d$. The step size in the analysis is one-tenth of L_d. Based on our calculations with different array and step size, and edge threshold intensity, the error incurred by dynamic window size is estimated to be less than 0.1% if the input timing step size is less than 15% of the input pulsewidth. The modified algorithm speeds up the simulation up to twofold when the total computed fiber distance reaches $2000L_d$. The computation time is dominated by approximately the last half of the fiber when the pulsewidth is the largest; this explains why the increase in the computation speed is twofold (and not larger) in the modified algorithm.

To simplify the problem and extract the essential properties of the interaction between the SPM effect and the fiber dispersion, we first confined our attention to the most dominant dispersion and nonlinear term, i.e., only the second-order dispersion and SPM effect are included in the simulation. The DCF acts as an ideal dispersion compensator for the SMF link where SSMF provides anomalous GVD ($\beta_2 < 0$) and DCF provides normal GVD ($\beta_2 > 0$). We adjust the link dispersions $|\beta_2 L|$ to be equal and opposite for the SSMF and DCF, and we take the ratio of nonlinearity to dispersion $|\gamma/\beta_2|$ to be the same for SSMF and DCF. The amount of SPM and fiber dispersion is characterized by the nonlinearity factor N and dispersion length L_d, respectively. The single isolated input pulses are considered to be Gaussian shaped. Fig. 2(a) shows the pulse shape of the input and compressed output pulse for different values of input peak power ($N^2 = 0.01$, 0.09, and 0.25) from a postcompensated fiber link of a total length $L/L_d = 200$, 1000, and 2000, respectively. The figure clearly shows the deterioration in the pulses as N is increased. There is almost no effect for $N^2 = 0.01$. At $N^2 = 0.09$, SPM starts to degrade the pulse recompression. At $N^2 = 0.25$, the SPM disturbs the dispersion balance rapidly. The size of the SPM effect is large when N is high. Hence the SPM effect gives an upper bound on the maximum input peak power that can be used for the ultrashort pulse transmission in the postcompensated fiber link. Fig. 2(b) shows the output pulses for the isolated input pulse after they propagate through a precompensated link of total length $L/L_d = 200$, 1000, and 2000 for $N^2 = 0.01$, 0.09, and 0.25, respectively. The pulses are recompressed back nicely even after a long distance ($2000L_d$) with high input peak power at a fixed input pulsewidth ($N^2 = 0.25$). The output maintains roughly the same pulse shape as the input pulse and displays no appreciable SPM induced dispersion balance degradation for $N^2 < 0.25$.

Fig. 3 shows the plot of output peak intensity from both compensating scenarios with respect to the propagation distance for different values of N. For the precompensated link, the output peak power does not change much when N is less than 0.5. Combined with the result of Fig. 2(b), it indicates the SPM effect in a precompensated link is almost negligible at these power levels. Comparing the curves for $N = 0.1$ and $N = 0.5$ from the postcompensated link, we can see that there is almost 50% peak power reduction when N is increased to 0.5. As the propagation distance is extremely large corresponding to a very substantial broadening of the pulse in SSMF, the output peak power in the SSMF falls substantially. Much (but not all) of the nonlinearity occurs at the beginning of the fiber due to the substantial pulse broadening and reduction in the peak intensity as the pulse propagates. For $N > 0.5$ the compressed pulse deteriorates rapidly, since the input pulse breaks into two parts in the SSMF—one propagates as a soliton and the other as a dispersive wave. The dispersive waves are compensated at the DCF but the soliton part is completely spread out. The net result is a very rapidly distorting pulse. Clearly, the input power must be kept sufficiently low to avoid such effects for good data transmission. The above simulation provides us the general views of the SPM effect on the dispersion compensated link when large pulse stretching and recompression occurs. By appropriately scaling using the nonlinear factor N and dispersion length L_d, we can apply the simulation results to a wide range of input pulsewidths and fiber lengths. Note that the soliton energies ($N^2 = 1$) for pulse durations of 100 fs, 500 fs, and 1 ps in SSMF are 435, 87, and 43.5 pJ, respectively. Therefore, in this ultrashort pulsewidth range,

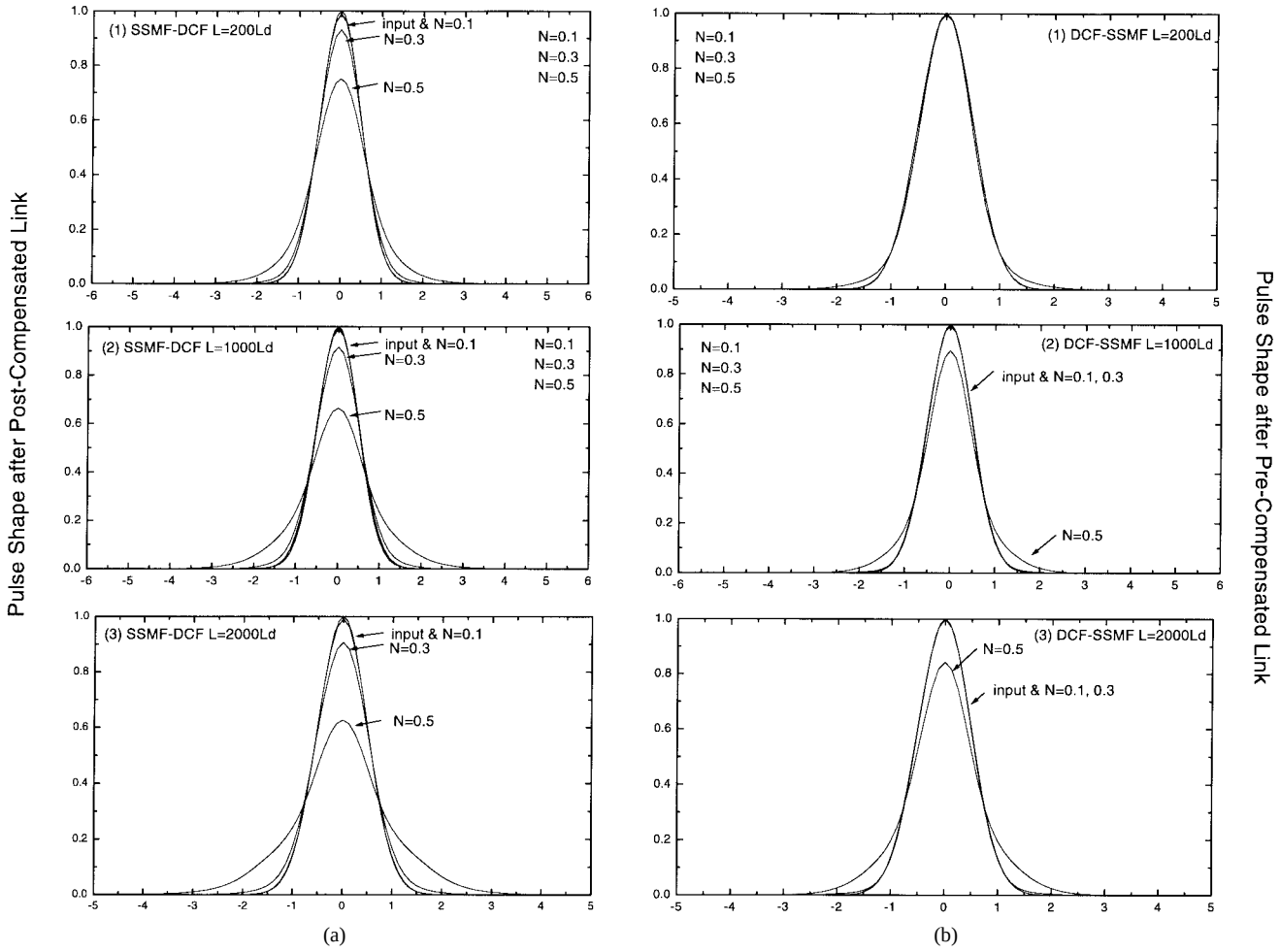

Fig. 2. (a) The simulated output pulse shape from a postcompensated link and (b) the simulated output pulse shape after a precompensated link.

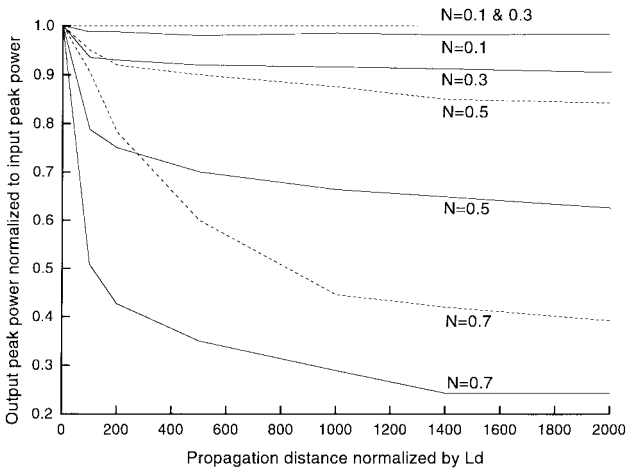

Fig. 3. The simulated output pulse intensity for a postcompensated link (solid line) and a precompensated link (dashed line) when $N = 0.1, 0.3, 0.5,$ and 0.7.

good transmission corresponding to $N^2 < 0.09$ is possible for energies well into the pJ range, which should be more than sufficient for high-quality communications even with a postcompensated link.

Another important feature of the SPM effect worth noticing is its different behavior in a postcompensated and a precompensated link. It is due to the asymmetric distribution of the anomalous GVD and normal GVD in the compensated link. In the postcompensating scenario, SPM introduces positive chirp in the propagating pulses and partially balances the effect of negative dispersion in the SSMF. The pulse broadening process is therefore slowed down. Since the size of the SPM effect is peak intensity dependent, the accumulated SPM effect is increased in the postcompensated link. In contrast, since the SPM effect accelerates the pulse broadening process in the initial DCF ($\beta_2 > 0$) of a precompensated link, the accumulated SPM is reduced due to the more rapidly reduced peak power. Thus, the precompensated link is more robust than a postcompensated link when input power is high. The output pulses from a precompensated link maintain a reasonable pulse shape and peak power even after a fiber link of $2000L_d$ when N^2 is 0.25. The power limit for a precompensated link thus could be further increased to nearly a hundred pJ for the fs-pulse transmission.

We noted that our simplified simulation includes only the second-order dispersion and the SPM term, where the parameters of DCF are the same as those of SSMF except the sign of the dispersion. Usually, the ratio of nonlinear coefficient γ to fiber dispersion β_2 is less for real DCF than for SSMF [26], [27]. Therefore, our simulation is conservative and overestimates the effect of SPM in the DCF. In our further analysis

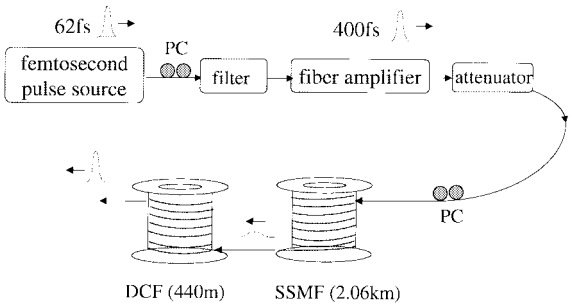

Fig. 4. Experiment setup for SPM effects on a 2.5-km dispersion compensated link. PC, polarization controller; filter, birefringent bandpass filter; fiber amplifier, chirped pulse fiber amplifier with maximum 20 dB gain; attenuator, fiber attenuator.

described in the following, we chose appropriate parameters for SSMF and DCF from our measurements and included the third-order dispersion, in order to match the simulation to the experiments. Finally, we noted the optimum DCF fiber length is different for linear and nonlinear pulse propagation. In our simulation and experiments, we focused on SPM effects with DCF fiber length optimized for linear compensation.

IV. Experiment and Simulation with Higher Order Dispersion

To verify our theoretical analysis, we performed experiments in a dispersion compensated link for isolated fs pulses with a fixed pulsewidth at different power levels. A 2.5-km transmission link consisting of a 2.06-km AT&T $5D$ single mode fiber and a 0.44-km DCF was built as the dispersion compensated link [10]. The SSMF has $D \approx 17$ ps/km/nm (or $\beta_2 \approx -22$ ps^2/km) and $D' \approx 0.05$ ps/km/nm^2 ($\beta_3 \approx 0.13$ ps^3/km) at 1550 nm taken from the spectral interferometry measurement [10]. The DCF has $D \approx -76$ ps/km/nm (or $\beta_2 \approx 98$ ps^2/km) measured by time-of-flight technique and a negative dispersion slope $D' \approx -0.2$ ps/km/nm^2 ($\beta_3 \approx -0.50$ ps^3/km) [10], [11]. The length ratio between SSMF and DCF is optimized for a nearly zero overall second-order dispersion. The residual dispersion slope of a 42-m concatenated link using such SSMF and DCF was estimated to be $\beta_3 \approx 0.0016 \pm 0.002$ ps^3/km ($D' \approx 0.0088 \pm 0.001$ ps/km/nm^2) by using the spectral interferometry technique [10]. It is roughly four times lower than the dispersion slope of DSF. The total loss of the 2.5-km compensated link, including splicing and connector losses, was measured to be 3 dB.

The experimental setup is shown in Fig. 4. The 62 fs pulses were generated from a stretched-pulse passively mode-locked fiber ring laser adopted from [28] at a repetition rate of ~33 MHz. The laser output was spectrally sliced by an interference filter ($\lambda_0 = 1559$ nm, FWHM = 9.8 nm) and amplified by a fiber amplifier [29] with output average power up to 5 mW. The input pulses for the transmission link were nearly bandwidth-limited (time-bandwidth product ~0.32) with pulsewidth of FWHM ~400 fs assuming secant-hyperbolic pulse shape and centered on $\lambda_0 = 1559$ nm. We adjusted the average power of the input pulses by a fiber pigtailed attenuator. The amount of SPM introduced in the transmission link can then be adjusted. The output pulse

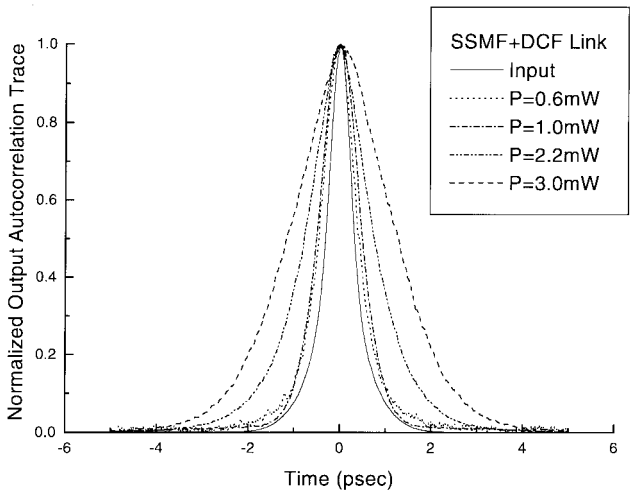

Fig. 5. Measured intensity autocorrelation traces of input and output pulses after a 2.5-km postcompensated link (normalized to unit amplitude). The input average power $P = 0.6, 1.0, 2.2$, and 3.0 mW with pulse repetition rate of 33 MHz. The input pulse FWHM is 400 fs (solid line).

intensity autocorrelation from the dispersion compensated link was measured at input average power ranging from 500 μW up to 3.5 mW. A fiber polarization controller was employed to optimize the polarization of input pulses for maximum autocorrelation signal. The input and output spectra of the link were compared through an optical spectrum analyzer (OSA). SPM effects on both precompensated (DCF-SSMF) link and postcompensated (SSMF-DCF) links were investigated.

Fig. 5 shows the input and output autocorrelation traces of the postcompensated link (SSMF-DCF) with input average powers of 0.6, 1.0, 2.2, and 3.0 mW, respectively. All the output autocorrelation traces shown were normalized to unit amplitude. The corresponding autocorrelation traces for the precompensated link are shown in Fig. 6. The power dependent output autocorrelation FWHM (not deconvolved) is shown in Fig. 7, from which the actual pulsewidths can be estimated by dividing the autocorrelation FWHM by 1.55 (assuming secant-hyperbolic pulse shape). The experiment is repeatable as indicated by the stable input pulsewidth (~400 fs) under each input power level shown in Fig. 7. It is clear that SPM effects behave in different ways in the postcompensated and precompensated cases as expected from our previous simulation results. For the postcompensated scenario, input pulses were initially stretched to ~200 ps (calculated) in the SSMF and recompressed back to ~500 fs (FWHM) in the subsequent DCF under linear low power operation (<500 μW or $N < 0.09$). The small output pulse broadening is due to the residual dispersion slope of the compensated link. The pulse broadening and recompression ratio is estimated be over 300. As the input power is increased from 500 μW to 3.5 mW with a corresponding pulse energy up to ~0.15 nJ, the pulse recompression was degraded by SPM effect significantly. The link output pulsewidth was broadened by almost a factor of three as shown in Fig. 7. As the input average power was further increased beyond ~3.5 mW (not shown), a soliton component was generated in SSMF, which was then broadened tremendously in the subsequent DCF. For the precompensated scenario, the positive dispersion of DCF balanced the negative

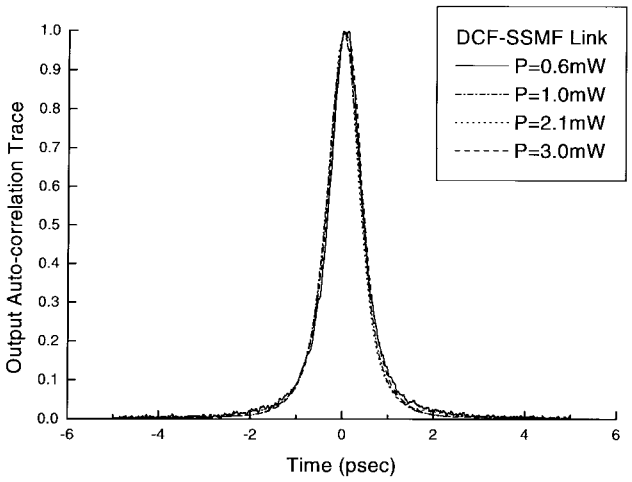

Fig. 6. Measured intensity autocorrelation traces of input and output pulses after a 2.5-km precompensated link (normalized to unit amplitude). The input average power $P = 0.6, 1.0, 2.1$, and 3.0 mW with pulse repetition rate of 33 MHz. The input pulse FWHM is 400 fs (solid line).

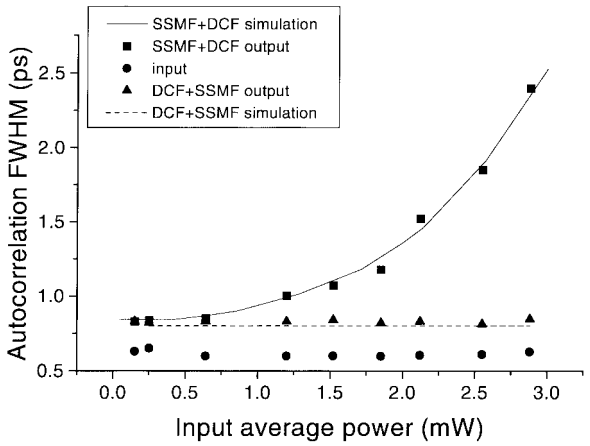

Fig. 7. Measured and simulation results of input and output pulse broadening due to the SPM effect in a 2.5-km dispersion compensated link. The input pulse FWHM is 400 fs.

dispersion of SSMF and recompressed the pulse back at the output end of the transmission link nicely. With input average power increased to as high as 3.5 mW, the output pulse width of the link does not change much. The SPM effect on the output pulses from a precompensated link is insignificant until much higher power levels.

Fig. 8 shows the input and output spectra width of the precompensated and postcompensated links. The input spectrum FWHM maintains the same ~6.5 nm for each measurement. A dramatic spectral narrowing effect was observed from the output of the postcompensated link when the input power was increased. By comparing the output spectra of the compensated link to the output spectra directly from SSMF, we observed that the spectral narrowing effect mainly (almost ~90%) occurred in the SSMF portion of the link. Subsequent to the SSMF, the optical pulse is negatively chirped and SPM leads to additional small spectral narrowing in the subsequent DCF. The latter result is consistent with the spectral narrowing effects previously observed from negatively chirped input pulses in normal dispersion fiber only [30]. For the precompensated

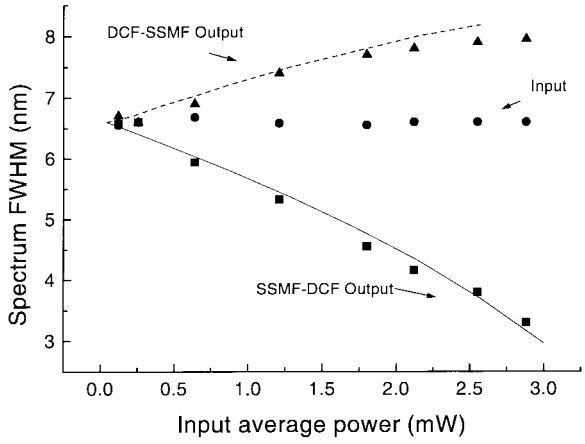

Fig. 8. Measured and simulation results of input and output pulse spectrum FWHM due to the SPM effect in a 2.5-km dispersion compensated link (solid line and dashed line: simulation results; circle, triangle, square: experiment data).

scenario, the output spectrum is slightly broadened when input power is increased up to 3 mW. Again, the effect of SPM on the output of the precompensated link is minor. For comparison, the results of simulations discussed later in detail are also shown in Figs. 7 and 8. Experimental data are in excellent agreement with the simulation.

To further investigate the actual output pulse shape of the link, we also measured the cross-correlation traces of the pulses. The reference pulse of the cross-correlation measurement was obtained from the fiber laser directly by splitting part of the laser output (FWHM = 62 fs) into the reference measurement path. In the cross-correlation measurement, the path of the signal pulses (2.5-km fiber) is much longer than that of the reference pulses (~2 m of free space). The $\#N$ output pulse was correlating with $\#N + 387$ instead of the $\#N$ reference pulse. The accuracy of cross-correlation measurement for the output of the 2.5-km transmission link is therefore limited to $\sim\pm 100$ fs by fiber laser timing jitter effects. In this experiment, the input is again maintained at 400 fs (FWHM) for each measurement assuming the secant-hyperbolic pulse shape. Fig. 9 shows cross-correlation traces of the postcompensated transmission link output when input power is 0.5, 2.0, and 3.2 mW, respectively. It was shown that the output pulse displays asymmetric oscillating tail even at low power. It indicates a small residual third-order dispersion of the concatenated link as expected from our previous experiment [10]. The output pulses were significantly broadened and deteriorated for the postcompensated link when input average power reaches 3.2 mW. Fig. 10 shows one example of a cross-correlation trace for the precompensated link when the input average power is high (3.2 mW). The output pulse broadening due to SPM is small. As a further metric of the effect of SPM, we calculated the ratio of output intensity to input intensity from our measured cross-correlation traces as shown in Fig. 11. The SPM induced peak power drop is almost 50%. These cross-correlation results are quantitatively consistent with the previous autocorrelation results.

To compare the experiment results with our theoretical analysis, we have performed numerical simulations corresponding

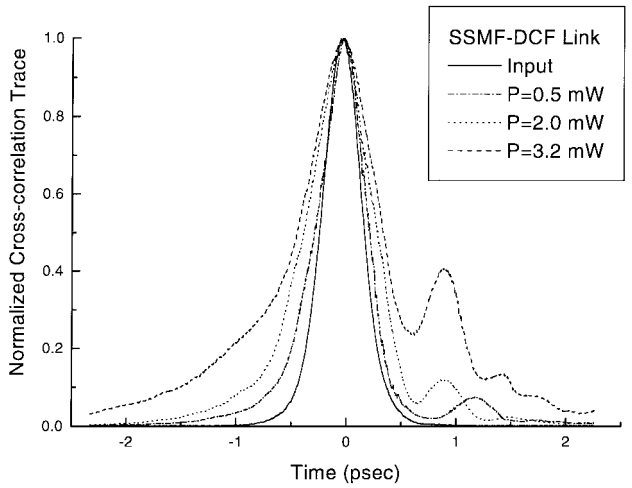

Fig. 9. Measured cross-correlation traces of input and output pulses after a 2.5-km postcompensated link (normalized to unit amplitude). The input average power $P = 0.5$, 2.0, and 3.2 mW with pulse repetition rate of 33 MHz. The input pulse FWHM is 400 fs (solid line).

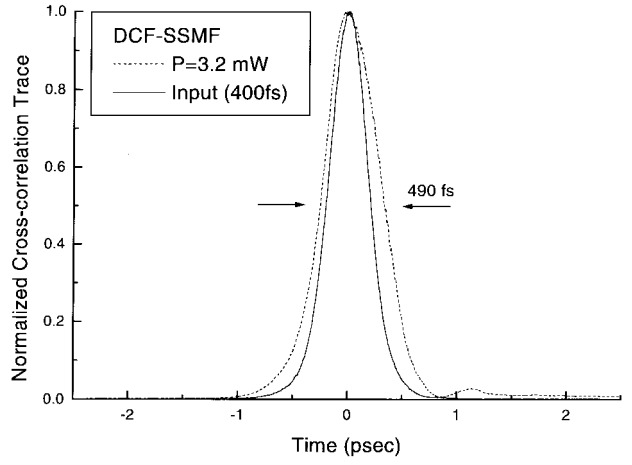

Fig. 10. Measured cross-correlation traces of input and output pulses after a 2.5-km precompensated link (normalized to unit amplitude). The input average power P is 3.2 mW at the pulse repetition rate of 33 MHz. The input pulse FWHM is 400 fs (solid line).

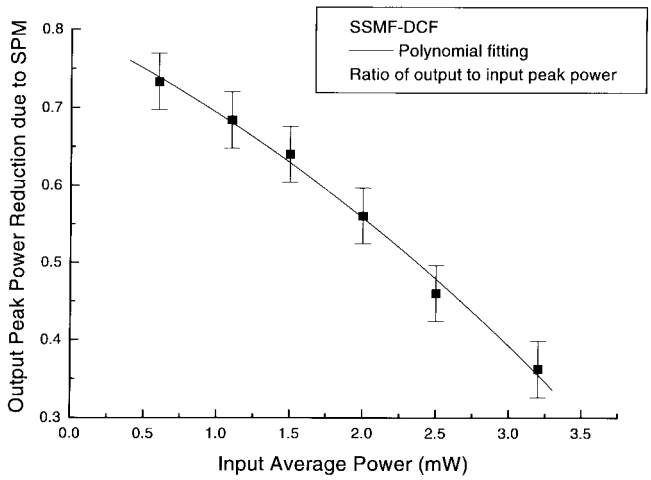

Fig. 11. The experiment result of peak power ratio of the output to input pulses in the postcompensated link due to the SPM effects. To clearly show the peak power reduction due to SPM, the output peak power used in calculating the power ratio is two times that of the actual measurement to account for the 3-dB loss of the transmission link. The input pulse FWHM is 400 fs (solid line).

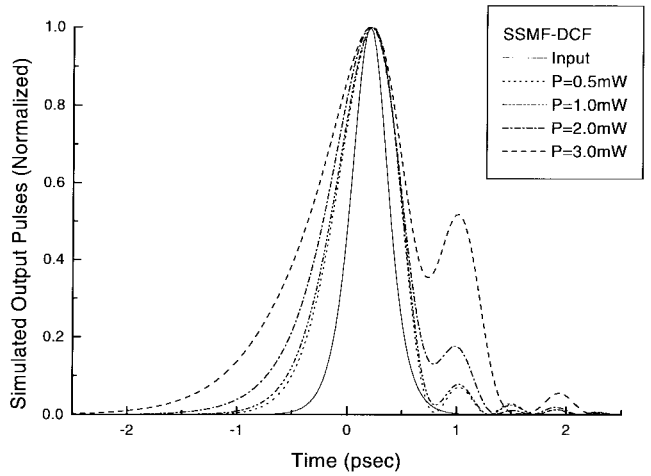

Fig. 12. Simulation results of normalized input and output pulses after a 2.5-km dispersion compensated link [SSMF (2.06 km)-DCF (0.44 km)] for input peak power $P_0 = 38$, 75, 150, and 230 mW. The input pulse FWHM is 400 fs (solid line).

to the experimental conditions. In contrast to the previous simulation where only the second-order dispersion and SPM are included, the third-order dispersion of SSMF and DCF were included in this simulation. The SSMF has $D = 17$ ps/km/nm (or $\beta_2 = -22$ ps^2/km) and $D' = 0.05$ ps/km/nm^2 at 1550 nm and the DCF has $D = -76$ ps/km/nm (or $\beta_2 = 98$ ps^2/km) and dispersion slope $D' = -0.2$ ps/km/nm^2. A small residual third-order dispersion was included in the analysis. The transmission link loss is mainly due to the fiber connector and splicing loss under our conditions. Therefore, the distributed fiber attenuation is lumped into connector loss in our model. The length of SSMF and DCF in the simulation was taken as 2.06 and 0.44 km, respectively. In our simulation, the nonlinear coefficient γ of SSMF was taken to be 1.2 W^{-1} km^{-1}, which is roughly consistent with measured results from [31] and [32]. The nonlinear coefficient γ of DCF was taken to be twice that of the SSMF. The ratio of nonlinear coefficient γ to fiber dispersion D for the DCF is comparable with reported values of other DCF's [26], [27]. These simulation parameters were confirmed by matching the simulated output spectra from either the SSMF (2.06 km) or the DCF (0.44 km) alone with the corresponding measured spectra, respectively. The input pulsewidth in the simulation is 400 fs with the secant hyperbolic pulse shape assumed. Fig. 12 shows the simulation results of SPM effects on the output pulse shape from a postcompensated link where the DCF is connected at the end of the SSMF. Fig. 13 shows SPM effects on the output pulse shape of a corresponding precompensated link. The output pulse shape after the transmission link under each input peak power level was normalized to unit amplitude. The precompensated link simulation is the same as that for postcompensated link except that the order of SSMF and DCF is reversed. In both cases, the small broadening in the output pulses under low power operation is due to the third-order dispersion mismatch of SSMF and DCF, which can

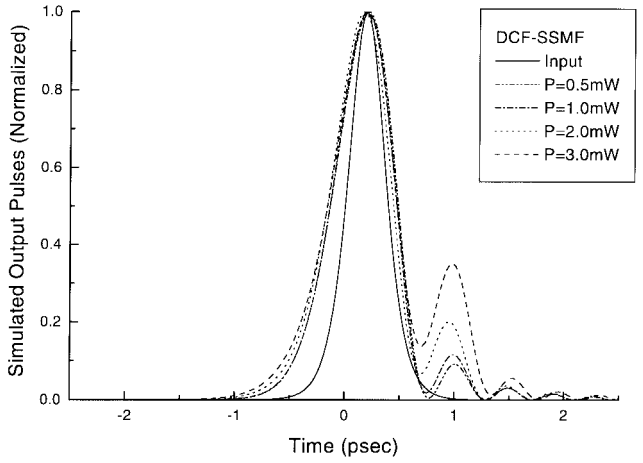

Fig. 13. Simulation results of normalized input and output pulses after a 2.5-km dispersion compensated link [DCF (0.44 km)-SSMF (2.06 km)] for input peak power $P_0 = 38, 75, 150$, and 230 mW. The input pulse FWHM is 400 fs (solid line).

be identified from the oscillating cubic tail of the output pulse shape. This simulation result is consistent with our cross-correlation trace measurement. The overall calculated pulse shape from the postcompensated link shows a great resemblance with the measured cross-correlation traces under various input powers. The measured cross-correlation traces from the precompensated link show less cubic tail than the corresponding simulation results, which is probably due to a small DCF nonlinear parameter mismatch between experiment and simulation. We also calculated the autocorrelation FWHM of the simulated output pulses with respect to input average power to match with our autocorrelation measurements shown in Fig. 7. The corresponding output spectra FWHM after the link was calculated as shown in Fig. 8. The simulation results of output pulsewidth and spectra width match the experiment data very well. This confirms that our theoretical approach is valid for the analysis of SPM effect on a dispersion compensated link in the fs regime when the pulse stretching and recompression is extremely large ($\sim$ on the order of several hundreds). By comparing this simulation with the previous simulation results which only consider the second-order dispersion and SPM, we noted that the second-order dispersion is the dominant term leading to the asymmetric behavior of SPM effects with respect to the postcompensated and precompensated links. Other effects, such as differences in loss and third-order dispersion of SSMF and DCF, are not needed to explain the overall trends.

We noted that our experiment and simulation results on isolated fs pulse transmission predict a better compensation performance in the precompensated link than the postcompensated link for high input average powers. Our results are consistent with previous TDM pulse transmission experiments where the pulse stretching and recompression ratio in the compensated link is small ($\sim$10) [14]–[16]. However, this contradicts the experiment reported in [18], where the postcompensated link shows a better compensation performance. This difference results because the DCF length in our work is selected for exact compensation at low input powers and the DCF fiber length in [18] appears to be optimized for partial compensation to accommodate the fiber nonlinearity.

V. Numerical Analysis of TDM Pseudorandom Data Transmission

We have experimentally and numerically demonstrated the SPM effects on a 400 fs pulse transmission over the dispersion compensated link using DCF. The isolated single pulse case is relevant to either ultrashort pulse CDMA schemes [16] or to fiber stretcher/compressor applications like chirped pulse amplification [19]. For CDMA schemes the previous analysis is an overly conservative estimate, since a coded input pulse will have substantially lower intensity for fixed energy than that of an uncoded input pulse considered above. To extend our theoretical model to TDMA transmission links, we performed simulations on pseudorandom fs pulse streams to investigate the applicability of linear propagation and dispersion compensation for ultrashort pulse TDM systems with extremely large pulse spreading and compression factors. The key difference here is that, as the pulses broaden, they overlap with neighboring pulses, so that the average power level remains approximately constant for further propagation. Therefore, unlike the case of an isolated pulse, nonlinear effects in TDMA transmission are expected to continue to accumulate roughly in proportion to the fiber length as the fiber span is increased. The exact intensity distribution, determined by the interference of the multiple overlapping pulses, is highly structured and varies rapidly along the fiber. Since the intensity distribution experienced by a particular bit is pattern dependent and also depends on the phase of the other nearby bits, this can result in an uneven distribution of nonlinear effects across different pulses. In the dispersion compensating process, this causes some bits to get overcompensated and others to get undercompensated.

Fig. 14 shows two examples of simulated eye diagrams for the TDM pulse transmission in a postcompensated link. The model only includes the second-order dispersion and SPM effects for the simulation. The dispersion slope term can be reasonably ignored as long as the pulsewidth is not too short ($>$500 fs). The input signal is a pulse sequence representing 128 bits, with "ones" and "zeros" chosen randomly. The pulses are Gaussian shaped with a bit separation equal to five times the FWHM pulsewidth ($\sim 0.83 T_0$), and the relative phase of one pulse with respect to the next is taken to be random. The bit stream was transmitted over $100 L_d$. Due to the wraparound property of the Fourier transform, the simulations treat the signal as an infinite bit sequence with a period of 128 bits. The effect of nonlinearity in this case is much stronger than in the isolated pulse cases. For $N^2 = 0.09$, the eye diagram is severely degraded and would result in a higher bit-error-rate for the fixed energy. Although some nonlinear effects still remain for $N^2 = 0.01$, the eye is wide open. For a 0.5-ps pulse, $N^2 = 0.01$ corresponds to a 0.87 pJ energy with the assumption outlined above. It implies that energy into a few-pJ range can be transmitted without a significant distortion, which is sufficient for high-quality communications. For longer fiber links, lower pulse energies should be used with

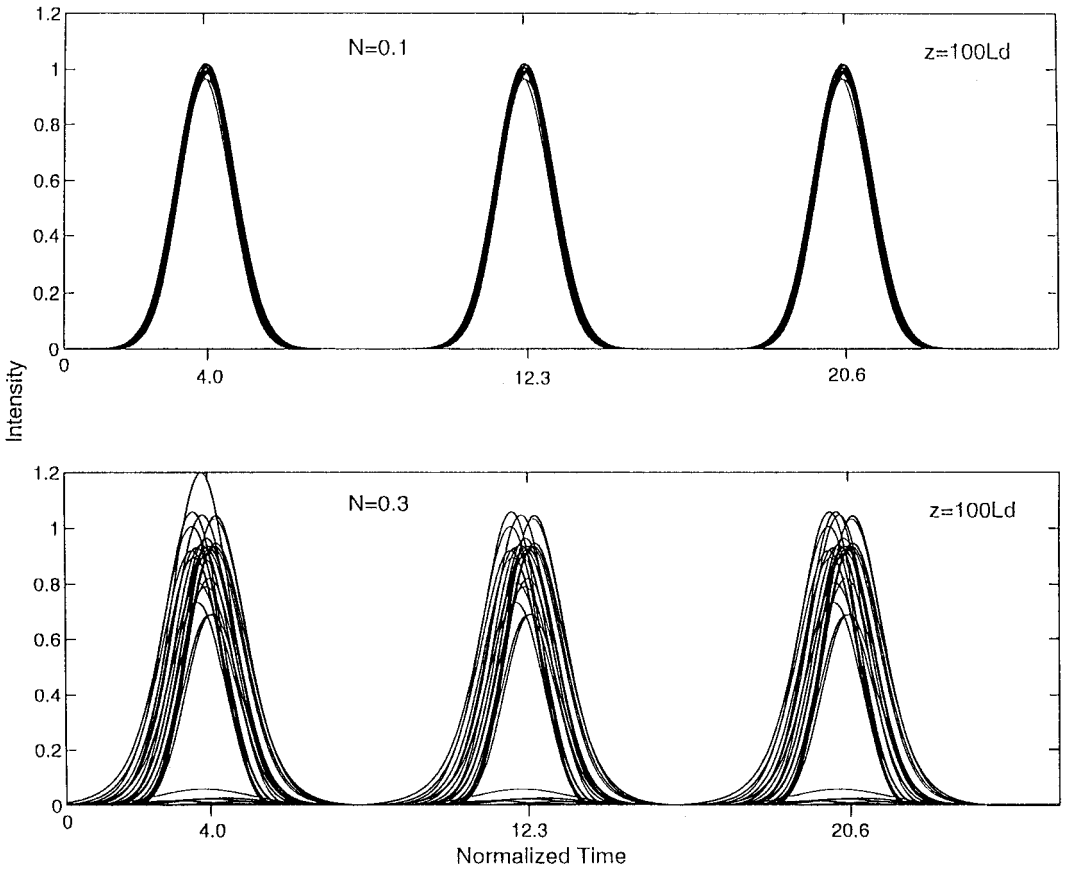

Fig. 14. Eye diagram of a 128-bit TDM pulse train separated by five times of pulsewidth propagating over $100L_d$ for $N = 0.1$ and 0.3.

permissible pulse energy expected to vary inversely with fiber length (assuming all other parameters held fixed).

VI. Summary

The interaction between the fiber dispersion and the SPM effect was shown to be a major factor that limits the amount of energy allowed to be launched into the dispersion compensated transmission link for fs pulses in our numerical and experimental study. This power limit will eventually provide an upper bound on the length of the transmission link due to the increasing loss for the longer link. Effects due to SPM are stronger for the postcompensated link. Nonetheless, our results indicate that transmission of sub-500 fs pulses in a dispersion-compensated fiber link should be possible at energy up to tens of pJ, which is consistent with high-quality communication. For the better pulse transmission, the precompensated scheme should be employed. We noted our result is overconservative for the CDMA pulse transmission where the spectrally coded pulse has much smaller peak power than the isolated unshaped input pulse. It is overly optimistic for the very high rate TDM pulse transmission when the pulse-to-pulse interactions can increase the nonlinearities compared to those that with a single isolated input pulse. Nevertheless, our study provides insight into the interaction between SPM and fiber dispersion in a dispersion compensated link for fs pulses. To our knowledge, this is the first numerical and experimental study of self-phase modulation in dispersion compensated fiber links for fs pulse transmission.

Acknowledgment

The authors gratefully acknowledge A. M. Vengsarkar and D. W. Peckham (Bell Laboratory) for supplying the dispersion compensating fiber and the single mode fiber used in the dispersion compensated link, and M. Newhouse and V. Da Silva of Corning Inc., for supplying erbium-doped fiber used in the fiber amplifier.

References

[1] S. Kawanishi, H. Takara, O. Kamatani, and M. Saruwatari, "200 Gbit/s 100 km time-division-multiplexed optical transmission using supercontinuum pulses with prescaled PPL timing extraction and all-optical demultiplexing," *Electron. Lett.*, vol. 31, pp. 816–817, 1995.

[2] J. A. Salehi, A. M. Weiner, and J. P. Heritage, "Coherent ultrashort light pulse code-division multiple access communication systems," *J. Lightwave Technol.*, vol. 8, pp. 478–491, 1990.

[3] S. Watanabe, T. Naito, and T. Chikama, "Compensation of chromatic dispersion in a single-mode fiber by optical phase conjugation," *IEEE Photon. Technol. Lett.*, vol. 5, pp. 92–95, 1993.

[4] R. M. Jopson, A. H. Gnauck, and R. M. Derosier, "10-Gb/s 360-km transmission over normal-dispersion fiber using mid-system spectral inversion," in *Proc. OFC'93 Tech. Dig.*, 1993, pp. 17–20.

[5] A. D. Ellis, M. C. Tatham, D. A. O. Davies, D. Nessett, D. G. Moodie, and G. Sherlock, "40 Gbit/s transmission over 202 Km of standard fiber using midspan spectral inversion," *Electron. Lett.*, vol. 31, pp. 299–301, 1995.

[6] R. Kashyap, S. V. Chernikov, P. F. Mckee, and J. R. Taylor, "30 ps chromatic dispersion compensation of 400 fs pulses at 100 Gbits/s in optical fibers using an all fiber photoinduced chirped reflection grating," *Electron. Lett.*, vol. 30, pp. 1078–1080, 1994.

[7] L. Dong, M. J. Cole, A. D. Ellis, M. Durkin, M. Ibsen, V. Gusmeroli, and R. I. Laming, "40 Gbit/s 1.55 nm transmission over 109 km of nondispersion shifted fiber with long continuously chirped fiber grating," in *Proc. OFC'97 Tech. Dig.*, 1997, paper PD-6, pp. 391–394.

[8] M. Stern, J. P. Heritage, and E. W. Chase, "Grating compensation of third-order fiber dispersion," *IEEE J. Quantum Electron.*, vol. 28, pp. 2742–2748, 1992.
[9] J. M. Dugan, A. J. Price, M. Ramadan, D. L. Wolf, E. F. Murphy, A. J. Antos, D. K. Smith, and D. W. Hall, "All-optical fiber-based 1550-nm dispersion compensation in a 10 Gbit/s, 150 km transmission experiment over 1310 nm optimized fiber," in *Proc. OFC'92 Tech. Dig.*, 1992, paper PD-14.
[10] C. C. Chang and A. M. Weiner, "Fiber transmission for sub-500-fs pulses using a dispersion-compensating fiber," *IEEE J. Quantum Electron.*, vol. 33, pp. 1455–1464, 1997.
[11] A. M. Vengsarkar, A. E. Miller, M. Haner, A. H. Gnauck, W. A. Reed, and K. L. Walker, "Fundamental-mode dispersion-compensating fibers: Design consideration and experiments," in *Proc. OFC'94 Tech. Dig.*, 1994, paper THK2, vol. 4, p. 225.
[12] C. Lin, H. Kogelnik, and L. G. Cohen, "Optical-pulse equalization of low-dispersion transmission in single-mode fibers in the 1.3–1.7 mm spectral region," *Opt. Lett.*, vol. 5, pp. 476–478, 1980.
[13] C. C. Chang, A. M. Weiner, A. M. Vengsarkar, and D. W. Peckham, "Broadband fiber dispersion compensation for sub-100-fs pulses with a compression ratio of 300," *Opt. Lett.*, vol. 21, pp. 1141–1143, 1996.
[14] M. Schiess, "Comparison of dispersion compensation schemes including fiber nonlinearities," *J. Opt. Commun.*, vol. 16, pp. 92–98, 1995.
[15] A. Berntson, D. Anderson, M. Lisak, M. L. Quiroga-Teixeiro, and M. Karlsson, "Self phase modulation in dispersion compensated optical fiber transmission systems," *Opt. Commun.*, vol. 130, pp. 153–162, 1996.
[16] F. Kuppers, A. Mattheus, and R. Ries, "Optimized design of passive fiber compensated transmission systems in view of Kerr nonlinearity," *Pure Appl. Opt.*, vol. 4, pp. 459–467, 1995.
[17] M. Stern, J. P. Heritage, R. N. Thurston, and S. Tu, "Self-phase modulation and dispersion in high data rate fiber-optic transmission systems," *J. Lightwave Technol.*, vol. 8, pp. 1009–1016, July 1990.
[18] R. Ludwig, W. Pieper, H. G. Weber, D. Breuer, K. Petermann, F. Kuppers, and A. Mattheus, "Unrepeatered 40 Gbit/s RZ single channel transmission over 150 km of standard single mode fiber at 1.55 mm," *Electron. Lett.*, vol. 33, pp. 76–77, 1997.
[19] C. C. Chang and A. M. Weiner, "Dispersion compensation for ultrashort pulse transmission using two-mode fiber equalizers," *IEEE Photon. Technol. Lett.*, vol. 6, pp. 1392–1394, 1994.
[20] C. C. Chang, H. P. Sardesai, and A. M. Weiner, "Code-division multiple-access encoding and decoding of femtosecond optical pulses over a 2.5-km fiber link," *IEEE Photon. Technol. Lett.*, vol. 10, pp. 171–173, 1998.
[21] M. D. Perry, Y. Ditmire, and B. C. Stuart, "Self-phase modulation in chirped-pulse amplification," *Opt. Lett.*, vol. 19, pp. 2149–2151, 1994.
[22] J. D. Minelly, A. Galvanauskas, M. E. Fermann, D. Harter, J. E. Caplen, Z. J. Chen, and D. N. Payne, "Femtosecond pulse amplification in cladding-pumped fibers," *Opt. Lett.*, vol. 20, pp. 1797–1799, 1995.
[23] W. J. Tomlinson, R. H. Stolen, and C. V. Shank, "Compression of optical pulses chirped by self-phase modulation in fibers," *J. Opt. Soc. Amer. B*, vol. 1, pp. 139–149, 1984.
[24] J. P. Gordon, "Dispersive perturbations of solitons of the nonlinear Schrofinger equation," *J. Opt. Soc. Amer. B*, vol. 9, pp. 91–97, 1992.
[25] G. P. Agrawal, *Nonlinear Fiber Optics*, 2nd ed. San Diego, CA: Academic, 1995, ch. 11.
[26] V. L. D. Silva, Y. M. Liu, A. J. Antos, G. E. Berkey, and M. A. Newhouse, "Comparison of nonlinear coefficient of optical fibers at 1550 nm," in *Proc. OFC'96 Tech. Dig.*, 1996, pp. 202–203.
[27] T. Kato, Y. Suetsugu, M. Takagi, E. Sasaoka, and M. Nishimura, "Measurement of the nonlinear refractive index in optical fiber by the cross-phase-modulation method with depolarized pump light," *Opt. Lett.*, vol. 9, pp. 988–990, 1995.
[28] K. Tamura, H. A. Haus, and E. P. Ippen, "Self-starting additive pulse mode-locking erbium fiber ring laser," *Electron. Lett.*, vol. 28, pp. 2226–2228, 1992.
[29] H. P. Sardesai and A. M. Weiner, "Nonlinear fiber-optic receiver for ultrashort pulse code division multiple access communications," *Electron. Lett.*, vol. 33, pp. 610–611, 1997.
[30] M. Oberthaler and R. A. Hopfel, "Special narrowing of ultrashort laser pulses by self phase modulation in optical fibers," *Appl. Phys. Lett.*, vol. 63, no. 8/23, pp. 1017–1019, 1993.
[31] K. S. Kim, R. H. Stolen, W. A. Reed, and K. W. Quoi, "Measurement of the nonlinear index of silica-core and dispersion-shifted fibers," *Opt. Lett.*, vol. 19, pp. 257–259, 1994.
[32] R. H. Stolen, K. S. Kim, S. E. Evangelides, G. T. Harvey, and W. A. Reed, "Nonlinear-index measurement by SPM at 1.55 mm," in *Proc. OFC'95 Tech. Dig.*, 1995, pp. 312–313.

Shuai Shen (M'98) was born in Beijing, Republic of China. He received the B.S. and M.S. degrees in applied physics from Tsinghua University, Republic of China, in 1992 and 1995, respectively. He is currently pursuing the Ph.D. degree in electrical engineering at Purdue University, West Lafayette, IN.

His research interests include high-speed optical communications, femtosecond pulse shaping, and optical sensor design based on surface plasmon resonance.

Mr. Shen is a member of the Optical Society of America (OSA).

Cheng-Chen Chang, photograph and biography not available at the time of publication. bio not provided.

Harshad P. Sardesai was born in Bombay, India. He received the B.E. degree from the University of Bombay, India, the M.S. degree from the University of Texas at Arlington, TX, and the Ph.D. degree from Purdue University, West Lafayette, IN, all in electrical engineering.

In October 1997, he joined Ciena Corporation, Linthicum, MD, where he is involved in the research and development of high data rate WDM systems. His research interests include lightwave system design, dispersion compensation, and ultrafast optics.

Vikrant Binjrajka, photograph and biography not available at the time of publication.

Andrew M. Weiner (M'84–SM'91–F'95) was born in Boston, MA, in 1958. He received the Sc.D. degree in electrical engineering from the Massachusetts Institute of Technology (M.I.T.), Cambridge, in 1984. His doctoral thesis, for which he was awarded the 1984 Hertz Foundation Doctoral Thesis Prize, dealt with femtosecond pulse compression (including generation of the shortest optical pulses reported up to that time) and measurement of femtosecond dephasing in condensed matter.

From 1979 to 1984, he was a Fannie and John Hertz Foundation Graduate Fellow at M.I.T. In 1984, he joined Bellcore, Holmdel, NJ, where he conducted research on ultrafast optics, including shaping of ultrashort pulses, nonlinear optics and switching in fibers, and spectral holography. In 1989, he became Manager of the Ultrafast Optics and Optical Signal Processing Research District. He assumed his current position as Professor of Electrical and Computer Engineering at Purdue University, West Lafayette, IN, in October 1992. Since August 1996, he has also been serving as Director of Graduate Admissions for the School of Electrical and Computer Engineering. His current research interests center on holography of ultrashort pulses, high-speed optical communications, applications of pulse shaping to femtosecond spectroscopy and nonlinear optics, and optical imaging in scattering media. He has published approximately 80 journal articles in the area of ultrafast laser optics and fiber communications and has been author or coauthor of over 150 conference papers in this field. He also is holder of five U.S. patents.

Dr. Weiner has served on numerous research review panels, professional society award committees, and conference program committees. He was Co-Chair of the 1996 and 1998 Conference on Lasers and Electro-optics, and Chair of the 1999 Gordon Conference on Nonlinear Optics and Lasers. In 1988-1989, he served as IEEE Lasers and Electro-Optics Society (LEOS) Traveling Lecturer. In addition, he has served as Associate Editor for IEEE JOURNAL OF QUANTUM ELECTRONICS, IEEE PHOTONICS TECHNOLOGY LETTERS, and *Optics Letters*. He was awarded the Adolph Lomb Medal of the Optical Society of America for pioneering contributions to the field of optics made before the age of 30. He was also awarded the 1997 Curtis McGraw Research Award of the American Society of Engineering Education and the 1997 International Commission on Optics Prize. He is a Fellow of the Optical Society of America (OSA). He is presently a member of the Board of Governors of the IEEE Lasers and Electro-Optics Society.